The 9th European Congress on Computational Methods in Applied Sciences and Engineering
ECCOMAS Congress 2024
3–7 June 2024, Lisboa, Portugal

A MIXED HYBRID-STRESS VIRTUAL ELEMENT FOR PLANE ELASTICITY

FRANCESCO S. LIGUORI[1], ANTONIO MADEO[1], SONIA MARFIA[1] AND ELIO SACCO[3]

[1] University of Calabria, DIMES
Ponte P. Bucci Arcavacata di Rende, CS, Italy
e-mail: francesco.liguori@unical.it, antonio.madeo81@unical.it

[2] Roma Tre University, DICITA
Via Vito Volterra 62, RM, Italy
email: sonia.marfia@uniroma3.it

[3] University of Naples Federico II, DiSt
Via Claudio 21, NA, Italy
email: elio.sacco@unina.it

Key words: Virtual elements, assumed stress, Hellinger Reissner, mixed finite elements

Summary. In this work, we introduce a hybrid variational framework for the Virtual Element Method (VEM) and develop a family of polygonal elements for plane elasticity. Under specific assumptions, it is demonstrated that the minimization of Total Potential Energy and the projection operation characteristic of enhanced VEM can be derived from the stationary condition of the Hellinger-Reissner mixed functional. The designed elements, which can be interpreted as either enhanced VEM or hybrid finite elements, are termed the Hybrid Virtual Element Method (HVEM). The primary variables in this approach are the displacements along the element boundary and the stress field within the element domain. The assumed stress field is represented on a polynomial basis that satisfies the divergence-free condition. In the HVEM formulation, stabilization-free elements are achievable using two concepts: *hyper-stability* and *iso-stability*. Notably, the *iso-stable* cases yield the most accurate recovery of both displacement and stress fields. The proposed HVEM family demonstrates high accuracy, even when coarse meshes are employed.

1 INTRODUCTION

The Virtual Element Method (VEM) is an innovative and original formulation belonging to the wide family of the Finite Element Method (FEM) [1]. The term "virtual" in VEM refers to the fact that the method does not explicitly assign the approximation form of the unknown field. In solid mechanics applications, the main feature of VEM is that the displacement field is not given explicitly in the internal element, but is specified only on its boundary [2, 3]. Therefore, the displacements of the nodes on the element boundary are the unknowns of the problem. Moreover, depending on the approximation hypotheses assumed, weighted averages of the displacements can be introduced as further unknowns of the problem. Because of the lack

of the explicit displacement field form, the strain is recovered adopting a projection procedure which (generally) requires the use of a stabilization term in the internal energy [4].

The VEM has been successfully used to solve linear elastic problems as well as nonlinear problems including plasticity, viscoelasticity, shape memory material behavior, and damage [5, 6]. Thanks to its mesh flexibility, VEM is adopted in contact mechanics [7] and in fracture mechanics where the element splitting technique is easily employed with successful results [8, 9].

The advances on the VEM formulation have concerned the development of new elements for different structural models and the proposal of new and efficient stabilization procedures [10] to address the numerical stability and enhance the convergence properties for a wide range of problems. In this context, a very challenging topic is the possibility of developing high-performance VEM formulations that do not require stabilization procedures [11, 12].

The standard VEM formulation is based on the approximation of the displacement along the element boundary through a piecewise k-th polynomial degree and on the assumption of a p-th polynomial degree representation of the strain field within the element, with $p = k - 1$. The strain field inside the element domain is obtained through a L_2 projection of the compatible strain. A modification of such a recipe has been proposed in D'Altri et al. [11]. Called enhanced VEM, this approach assumes a polynomial degree p different from $k - 1$ and proposes the adoption of an energy norm projection. The adoption of the energy norm implicitly leads to the introduction of an approximation of the stress field, which suggests that the enhanced VEM construction could make use of a mixed or hybrid formulation of the boundary value problem. Hence, VEM approaches based on mixed variational formulations have been recently proposed and discussed [13, 14, 15, 16].

Mixed approaches have been extensively used in the formulation of high-performance finite elements. In such cases, starting from a mixed variational principle, the stress or the strain fields are taken as primary variables together with the displacements. The main advantages demonstrated by the mixed FEM are the improvement of the overall accuracy, the elimination of various locking phenomena and the enchantment of the stress and strain representation [17]. Within the mixed FEM, an interesting approach is represented by the hybrid formulation. Being based on assumed stress fields that a-priori satisfy the equilibrium equations, it allows the displacement field to be interpolated only along the element boundary. Among the others, a quadrilateral membrane hybrid finite element with drilling rotations and no spurious modes has been proposed in [18]. The element is formulated within the Hellinger-Reissner variational principle and assumes a stress approximation implicitly satisfying the equilibrium equations with zero bulks loads. Additionally, the assumed stress is defined as isostatic, namely it is ruled by a number of stress parameters that exactly matches the number of kinematical deformation modes. Since these elements do not require the assumption of the displacement field inside the element domain, they exhibit many similarities with VEM formulations.

Hybrid membrane finite elements have also been developed by assuming stresses that satisfy both equilibrium with zero bulks loads and compatibility equations [19]. This stress assumption allows the finite element operators to be evaluated only by performing boundary integration. The hybrid FEM has also been used to setup linear elastic shell elements with four nodes [20] or eight nodes [21]. These elements in general exhibit high accuracy for rough meshes and the same rate of convergence for both displacements and stresses solutions. This behavior has also been confirmed for composite materials applications and for geometrically nonlinear problems [22]. Finally, good performance has been observed when hybrid FEM is used in the context of

plasticity problems [23]. The possibility of integrating the element operators along the boundary facilitates the formulation of polygonal hybrid elements [24].

In the present paper it is proved that the enhanced VEM formulation proposed in [11] can be recognized as a special hybrid finite element model under specific assumptions. Thus, the aim of the paper is to propose a family of elements, named Hybrid Virtual Element Method (HVEM), because they can be regarded as enhanced VEM or as hybrid FEM.

A rational procedure for defining different strain field bases for the HVEM is provided, considering the number of degrees of freedom (DOF) and of rigid motions of the element (3 in-plane), with the objective of recovering self-stabilized elements. One of the main drawback of the VEM, occurring when the degree p of the strain field polynomial approximation is increased, is the arising of new internal unknowns of the element; a technique for avoiding this bother is discussed for the HVEM. Moreover, the problem of defining a minimal basis for the strain field, denoted as the *iso-stable* basis, that ensures the element stability, is approached.

A numerical application is presented in order to assess the efficiency of the proposed HVEM. Additional details on the HVEM approach can be found in [25]. Furthermore, stabilization-free HVEM has been successfully adopted in plasticity problems in [26].

2 BASIC EQUATIONS

Let a body Ω be considered, subjected to body forces $\boldsymbol{b}$, with boundary split into two parts: Γ_p, where the traction $\boldsymbol{p}$ is specified, and Γ_u, where the displacement field $\bar{\boldsymbol{u}}$ is prescribed, so that $\Gamma = \Gamma_p \cup \Gamma_u$ and $\Gamma_p \cap \Gamma_u = 0$. A Cartesian coordinate system $\{O, x_1, x_2\}$ is introduced.

In the framework of small strain and small displacement theory, the field governing equations of the 2D elasticity boundary value problem (BVP), i.e. the strain-displacement relationship, the equilibrium equation and the constitutive law, are:

$$\begin{cases} \boldsymbol{\varepsilon} = \boldsymbol{D}\boldsymbol{u} \\ \boldsymbol{D}^T\boldsymbol{\sigma} + \boldsymbol{b} = \boldsymbol{0} \qquad \text{in } \Omega \\ \boldsymbol{\sigma} = \boldsymbol{C}\boldsymbol{\varepsilon} \end{cases} \tag{1}$$

with the boundary conditions:

$$\begin{array}{lcll} \boldsymbol{N}\,\boldsymbol{\sigma} & = & \boldsymbol{p} & \text{on } \Gamma_p \\ \boldsymbol{u} & = & \bar{\boldsymbol{u}} & \text{on } \Gamma_u \end{array} \tag{2}$$

In Eqs. (1) and (2), the classical Voigt notation is adopted, with $\boldsymbol{D}$ the compatibility differential operator, $\boldsymbol{N}$ the matrix of the unit normal to Γ.

The total potential energy can be written as:

$$\Pi[\boldsymbol{u}] = \Phi[\boldsymbol{u}] - \mathcal{W}[\boldsymbol{u}] \tag{3}$$

where the external work is defined as:

$$\mathcal{W}[\boldsymbol{u}] = \int_\Omega \boldsymbol{b}^T\boldsymbol{u}\, dA + \int_{\Gamma_p} \boldsymbol{p}^T\boldsymbol{u}\, ds \tag{4}$$

the displacement field satisfies the boundary condition in Eq. $(2)_2$, the stress field is $\boldsymbol{\sigma}[\boldsymbol{u}] = \boldsymbol{C}(\boldsymbol{D}\boldsymbol{u})$ and the internal strain energy is:

$$\Phi[\boldsymbol{u}] = \frac{1}{2}\int_\Omega \boldsymbol{\varepsilon}^T[\boldsymbol{u}]\boldsymbol{C}\boldsymbol{\varepsilon}[\boldsymbol{u}]\, dA. \tag{5}$$

The Hellinger-Reissner variational functional is expressed as:

$$\Pi_{HR}[\boldsymbol{u},\boldsymbol{\sigma}] = \Phi_d[\boldsymbol{u},\boldsymbol{\sigma}] - \Phi_c[\boldsymbol{\sigma}] - \mathcal{W}[\boldsymbol{u}], \tag{6}$$

where

$$\Phi_d[\boldsymbol{u},\boldsymbol{\sigma}] = \int_\Omega \boldsymbol{\sigma}^T \boldsymbol{D}\boldsymbol{u}\, dA, \quad \Phi_c[\boldsymbol{\sigma}] = \frac{1}{2}\int_\Omega \boldsymbol{\sigma}^T \boldsymbol{C}^{-1}\boldsymbol{\sigma}\, dA, \tag{7}$$

and the displacement field satisfies the boundary condition in Eq. $(2)_2$. For convenience, by applying the diverge theorem, the internal work Φ_d can be split into a domain and a boundary contribute as

$$\Phi_d = \int_\Gamma (\boldsymbol{N}\boldsymbol{\sigma})^T \tilde{\boldsymbol{u}}\, ds - \int_\Omega (\boldsymbol{D}^T\boldsymbol{\sigma})^T \boldsymbol{u}\, dA. \tag{8}$$

3 VEM FORMULATION

The first step of the formulation of VEM consists in the discretization of the domain Ω in n_e subdomains, i.e. elements, Ω_e. Within each element Ω_e the displacement field $\boldsymbol{u}$ is approximated as $\boldsymbol{u}^h$, whose explicit expression is not defined; the trace of the displacement field $\boldsymbol{u}^h$ on the boundary of the element Γ_e is denoted as $\tilde{\boldsymbol{u}}^h$ and an explicit representation of this field is given:

$$\tilde{\boldsymbol{u}}^h = \boldsymbol{N}_b\, \hat{\boldsymbol{u}} \tag{9}$$

where $\hat{\boldsymbol{u}}$ is the vector of the nodal displacements on Γ_e; considering n nodes on the element boundary, the size of the vector $\hat{\boldsymbol{u}}$ is $2\,n$. Moreover, $\boldsymbol{N}_b$ is the $2 \times 2\,n$ matrix of the polynomial functions. The components of the displacement vector $\hat{\boldsymbol{u}}$ represent the unknowns of the approximated form of the BVP.

According to the the classical procedure for the construction of VEM, as the displacement field is not explicitly given in Ω_e, it is not possible to derive the strain by the compatibility equation, so that the strain-displacement relationship needs to be relaxed. In fact, the consistent approximated strain is evaluated as the projection of the (unknown) compatible strain on a subspace of polynomial function with a given degree of the power. In formula, the strain is represented as:

$$\boldsymbol{\varepsilon}^h = \boldsymbol{N}_\varepsilon\, \hat{\boldsymbol{\varepsilon}} \tag{10}$$

with $\boldsymbol{N}_\varepsilon$ the matrix of the p degree of polynomial functions representing the basis for the strain approximation and $\hat{\boldsymbol{\varepsilon}}$ vector of strain parameters. The approximated strain can be evaluated by enforcing a minimal distance (in a chosen norm) between $\boldsymbol{\varepsilon}^h$ and $\boldsymbol{D}\boldsymbol{u}^h$.

3.1 Mixed energy

A mixed energy norm can be adopted, observing that the terms $\boldsymbol{C}\,\boldsymbol{\varepsilon}^h$ and $\boldsymbol{C}\,\boldsymbol{D}\boldsymbol{u}^h$ from a mechanical point of view are stresses. Thus, the approximated stress field $\boldsymbol{\sigma}^h$ is introduced and represented as:

$$\boldsymbol{\sigma}^h = \boldsymbol{N}_\sigma\, \hat{\boldsymbol{\sigma}}. \tag{11}$$

Taking into account Eq. (11), one obtains:

$$\min_{\hat{\boldsymbol{\sigma}}} \int_{\Omega_e} \left(\boldsymbol{C}^{-1}\boldsymbol{N}_\sigma\, \hat{\boldsymbol{\sigma}} - \boldsymbol{D}\boldsymbol{u}^h\right)^T \left(\boldsymbol{N}_\sigma\, \hat{\boldsymbol{\sigma}} - \boldsymbol{C}\,\boldsymbol{D}\boldsymbol{u}^h\right) dA. \tag{12}$$

Introducing the definitions:

$$\boldsymbol{G}_\sigma = \int_{\Omega_e} \left(\boldsymbol{C}^{-1}\,\boldsymbol{N}_\sigma\right)^T \boldsymbol{N}_\sigma\, dA, \qquad \boldsymbol{B}_\sigma = \int_{\Gamma_e} \boldsymbol{N}_\sigma^T \boldsymbol{N}_e^T \boldsymbol{N}_b\, ds \tag{13}$$

and implicitly assuming that $\boldsymbol{N}_\sigma$ satisfies the relationship $\boldsymbol{D}^T\,\boldsymbol{N}_\sigma = \boldsymbol{0}$, the stationary condition of Eq. (12) leads to:

$$\boldsymbol{G}_\sigma \hat{\boldsymbol{\sigma}} = \boldsymbol{B}_\sigma \hat{\boldsymbol{u}}. \tag{14}$$

In such a case, the strain representation in Eq. (10) can be expressed as:

$$\boldsymbol{\varepsilon}^h = \boldsymbol{\Pi}_\sigma\,\hat{\boldsymbol{u}} \qquad \text{with } \boldsymbol{\Pi}_\sigma = \boldsymbol{C}^{-1}\,\boldsymbol{N}_\sigma\,\boldsymbol{G}_\sigma^{-1}\,\boldsymbol{B}_\sigma \tag{15}$$

where $\boldsymbol{\Pi}_\sigma$ is projector of the compatible strain field obtained through stress approximation.

3.2 Total potential energy formulation

Once the strain field is determined within the virtual element as a function of the displacement of the boundary nodes, the total potential energy in Eq. (3) is written and minimized with respect to the nodal displacement degrees of freedom.

Taking into account Eq. (15) for the projected strain, the stationarity condition of the total potential energy written at the element level takes the form:

$$\boldsymbol{0} = \boldsymbol{K}_\sigma\,\hat{\boldsymbol{u}} - \hat{\boldsymbol{b}} \tag{16}$$

where

$$\boldsymbol{K}_\sigma = \boldsymbol{B}_\sigma^T\,\boldsymbol{G}_\sigma^{-1}\left(\int_{\Omega_e} \boldsymbol{N}_\sigma^T\,\boldsymbol{C}^{-1}\,\boldsymbol{N}_\sigma\, dA\right)\boldsymbol{G}_\sigma^{-1}\,\boldsymbol{B}_\sigma = \boldsymbol{B}_\sigma^T\,\boldsymbol{G}_\sigma^{-1}\,\boldsymbol{B}_\sigma. \tag{17}$$

is the so-called (consistent) stiffness matrix, recovered by the stationary condition of the potential energy once an expression of the projected strain is considered. The vector $\hat{\boldsymbol{b}}$ is the equivalent element load vector accounting for traction and bulk load. It can be remarked that the enhanced VEM approach does not require the use of a stabilization term, as the matrix $\boldsymbol{N}_\sigma$ is properly set in order to ensure no spurious energy modes.

4 Hybrid formulation for VEM

In this Section, the equivalence between the enhanced VEM, based on the mixed energy formulation and a hybrid mixed FEM is proved, leading to the formulation of the HVEM. The special case of divergence-free interpolation is considered.

The hybrid FEM is based on the Hellinger-Reissner mixed variational formulation given by Eq. (6), taking into account Eqs. (7) and (8). Thus, both displacements $\boldsymbol{u}^h$ and stresses $\boldsymbol{\sigma}^h$ represent the unknowns of the BVP problem. The displacement is explicitly approximated on the boundary Γ_e by Eq. (9), while the stress is represented in the form given in Eq. (11) in each element, satisfying divergence-free condition. Thus, the Hellinger-Reissner energy, written at the single element level, becomes:

$$\Pi_{HR1}^e[\hat{\boldsymbol{u}}, \hat{\boldsymbol{\sigma}}] = \hat{\boldsymbol{\sigma}}^T \boldsymbol{B}_\sigma \hat{\boldsymbol{u}} - \frac{1}{2}\hat{\boldsymbol{\sigma}}^T\,\boldsymbol{G}_\sigma \hat{\boldsymbol{\sigma}} - \hat{\boldsymbol{u}}^T \hat{\boldsymbol{b}} \tag{18}$$

where the definitions, given in Eq. (13), have been taken into account.

The stationarity condition of the elemental Hellinger-Reissner energy (18), with respect to $\hat{\boldsymbol{u}}$ and $\hat{\boldsymbol{\sigma}}$, leads to the following algebraic equations:

$$\mathbf{0} = \boldsymbol{B}_\sigma^T \hat{\boldsymbol{\sigma}} - \hat{\boldsymbol{b}} \tag{19}$$

$$\mathbf{0} = \boldsymbol{B}_\sigma \hat{\boldsymbol{u}} - \boldsymbol{G}_\sigma \hat{\boldsymbol{\sigma}}. \tag{20}$$

It is worth noting that Eq. (20) exactly matches Eq. (14), recovered for the mixed energy formulation of the VEM projector. In fact, solving this compatibility equation and enforcing the constitutive equation, the strain field representation obtained for the VEM formulation in Eq.(15) is retrieved.

Substituting the stress vector parameters $\hat{\boldsymbol{\sigma}}$ obtained from Eq. (20) into the equilibrium equation (19), one obtains:

$$\mathbf{0} = \boldsymbol{B}_\sigma^T \, \boldsymbol{G}_\sigma^{-1} \, \boldsymbol{B}_\sigma \, \hat{\boldsymbol{u}} - \hat{\boldsymbol{b}}, \tag{21}$$

that exactly corresponds to Eq. (16) with $\boldsymbol{K}_\star = \boldsymbol{K}_\sigma$, obtained through the minimization of the total potential energy of the VEM mixed energy formulation.

5 STABILIZATION-FREE HVEM

5.1 Approximation of the element boundary displacement

An interpolation of the displacement field ruled by the displacements of nodes located at the geometrical vertexes of the polygonal element is considered. Therefore, the number of nodes n coincides with the number of edges of the polygonal shape.

A specific choice is made in the proposed elements consisting in a linear interpolation of the displacement field along the element boundary, i.e. the degree of the functions in $\boldsymbol{N}_b$ is $k = 1$. The assumed linear interpolation represents a common and useful choice, but higher order interpolations can be readily considered.

5.2 Stress field approximation

As declared in Section 3, the stress field inside the element is approximated by p degree polynomial functions. Thus, let the three components space $\mathcal{R}_p^3[x_1, x_2]$ representing polynomials of maximum degree p and variables $[x_1, x_2]$ be considered. It is possible to define the vectorial subspace $\mathcal{M}_p^3[x_1, x_2] \subseteq \mathcal{R}_p^3[x_1, x_2]$ which satisfies the equilibrium equations with zero bulk loads. A basis of $\mathcal{M}_p^3[x_1, x_2]$ up to the p-th polynomial order can be expressed as:

$$\mathcal{M}_p^3[x_1, x_2] = span([\mathcal{N}_0|\mathcal{N}_1|\mathcal{N}_2|\dots|\mathcal{N}_p]), \tag{22}$$

where each $\mathcal{N}_q$, with $q = 1, .., p$, represents divergence-free vectors of polynomials of order q.

The explicit expression of these matrices up to $p = 4$ is given in [25].

The space $\mathcal{M}_p^3[x_1, x_2]$ can be used to interpolate the stress field, as indicated in Eq. (11), so that $\boldsymbol{D}^T \boldsymbol{\sigma}^h = \mathbf{0}$. In particular, it is possible to select an appropriate subspace from $\mathcal{M}_p^3[x_1, x_2]$ whose dimension defines the number of stress parameters $\hat{\boldsymbol{\sigma}}$. This choice has a significant relevance on the element stability, that is defined as the absence of spurious modes in the element stiffness matrix $\boldsymbol{K}_\sigma$.

For a polynomial element with n nodes, the number of deformation modes is $m = 2n - 3$. As shown elsewhere in the context of quadrilateral FEs [27], a necessary condition for element

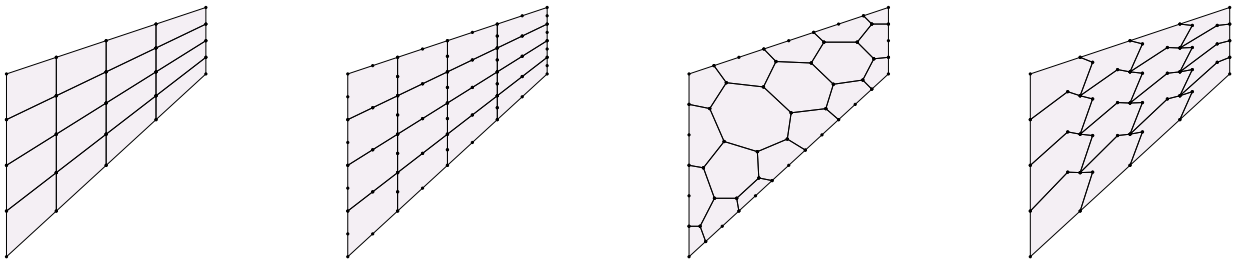

(a) M-str4 (b) M-str8 (c) M-poly (d) M-conc

Figure 1: Cook's membrane: mesh topologies.

stability is that the number of stress parameters should at least match the number of deformation modes, i.e. $\dim(\hat{\boldsymbol{\sigma}}) \geq m$. Once the necessary condition is satisfied, to prove element stability it is required that $\text{rank}(\boldsymbol{K}_\sigma) = m$ for all the possible element geometrical configurations.

The number of stress parameters, i.e. $\dim(\hat{\boldsymbol{\sigma}})$, defines two contexts for stability, named *hyper-stability* and *iso-stability*, both satisfying the stability condition $\text{rank}(\boldsymbol{K}_\sigma) = m$:

1. when $\dim(\hat{\boldsymbol{\sigma}}) \geq m$ and $\boldsymbol{N}_\sigma \equiv \mathcal{M}_p^3$ *hyper-stability* occurs in the element; in such a case, a complete polynomial order is used to interpolate the stresses and there may be redundancy in the number of stress parameters;

2. when $\dim(\hat{\boldsymbol{\sigma}}) = m$, the stress interpolation is ruled by the minimum number of stress parameters required for stability and *iso-stability* is obtained; in this case $\boldsymbol{N}_\sigma \subseteq \mathcal{M}_p^3$ and the polynomial order of the stress interpolation function may not be complete.

It is worth to remark that the concept of *iso-stability* coincides with that of isostatic assumed stress in mixed FEM, successfully employed in the analysis of membrane [27, 18] and shells in linear [21] and nonlinear contexts [28, 22].

The specific expression for the iso and hyper stable assumed stress fields can be found elsewere [25].

6 NUMERICAL RESULTS

A popular benchmark for assessing the performance of the proposed formulation in shear dominated problems is here analysed. The test concerns a tapered cantilever beam loaded by a shear force [25]. Elastic modulus and Poisson's ratio are $E = 1$ and $\nu = 0.333$, respectively. The structure is discretized using different mesh topologies, represented in Fig. 1.

Table 1 shows the results obtained using four noded structured meshes for displacements and principal stresses. For all the refinement levels, HVEM-iso proves to be more accurate than HVEM-hyp and the advantages in using HVEM-iso are more evident for the coarsest meshes. A similar trend can be observed in Table 2 for eight nodes elements. In this case, HVEM-iso is more accurate than HVEM-hyp in evaluating the displacement, while HVEM-hyp gives better stress results in the 2×2 case. Analogously, HVEM-iso gives better results than HVEM-hyp in Voronoi meshes for the vertical displacement in A and the maximum principal stress in C, as shown in Table 3. However, these results allow to highlight the high level of accuracy obtained

Table 1: Cook's membrane: Displacement in A (u_2^A), maximum principal stress in C (σ_{mx}^C) and minimum principal stress in B (σ_{mn}^B) for M-str4 meshes.

	mesh	2×2	4×4	8×8	16×16	32×32
u_2^A	HVEM-iso	22.3230	23.5160	23.8023	23.9107	23.9462
	HVEM-hyp	15.0387	20.6074	22.9487	23.6844	23.8873
	reference			23.960		
σ_{mx}^C	HVEM-iso	0.1381	0.1837	0.2133	0.2252	0.2310
	HVEM-hyp	0.1032	0.1669	0.2071	0.2243	0.2312
	reference			0.2362		
σ_{mn}^B	HVEM-iso	-0.2319	-0.1848	-0.2014	-0.2038	-0.2039
	HVEM-hyp	-0.1403	-0.1752	-0.1979	-0.2041	-0.2048
	reference			-0.2023		

Table 2: Cook's membrane: Displacement in A (u_2^A), maximum principal stress in C (σ_{mx}^C) and minimum principal stress in B (σ_{mn}^B) for M-str8 meshes.

	mesh	2×2	4×4	8×8	16×16	32×32
u_2^A	HVEM-iso	23.8734	23.9606	23.9754	23.9720	23.9690
	HVEM-hyp	23.6331	23.8925	23.9432	23.9584	23.9642
	reference			23.960		
σ_{mx}^C	HVEM-iso	0.2182	0.2311	0.2349	0.2362	0.2367
	HVEM-hyp	0.2201	0.2247	0.2295	0.2329	0.2349
	reference			0.2362		
σ_{mn}^B	HVEM-iso	-0.1448	-0.2043	-0.2080	-0.2045	-0.2038
	HVEM-hyp	-0.1526	-0.2018	-0.2020	-0.2027	-0.2031
	reference			-0.2023		

even for very coarse meshes, that represents one of the main advantages of adopting the HVEM formulation.

The convergence properties of the proposed HVEM using quadrilateral and polygonal meshes are compared in Fig. 2 (a). The results show that the rate of convergence is the same for quadrilateral and polygonal elements, while a better accuracy is obtained with M-poly meshes. The same comparison is performed considering an incompressible material, characterised by $\nu = 0.499999$ and a plane strain constitutive law.

The results, given in Fig. 2 (b), show that polygonal meshes provide a more accurate solution than the quadrilateral ones. Additionally, in both cases the HVEM formulation is compared with the 5β mixed FE. It can be observed that its performance are close to those provided by HVEM-iso. Finally, it is worth noting that the use of incompressible materials does not alter the performance of HVEM-iso and HVEM-hyp in terms of both accuracy ad rate of convergence.

Table 3: Cook's membrane: Displacement in A (u_2^A), maximum principal stress in C (σ_{mx}^C) and minimum principal stress in B (σ_{mn}^B) for M-poly meshes.

	dofs	18	88	272	914	3030
u_2^A	HVEM-iso	23.2370	23.7960	23.8990	23.9433	23.9600
	HVEM-hyp	21.5626	23.7015	23.8811	23.9409	23.9587
	reference			23.960		
σ_{mx}^C	HVEM-iso	0.2397	0.2229	0.2300	0.2357	0.2360
	HVEM-hyp	0.2242	0.2364	0.2328	0.2380	0.2377
	reference			0.2362		
σ_{mn}^B	HVEM-iso	-0.1813	-0.1903	-0.1982	-0.2012	-0.2028
	HVEM-hyp	-0.1979	-0.2082	-0.2068	-0.2028	-0.2047
	reference			-0.2023		

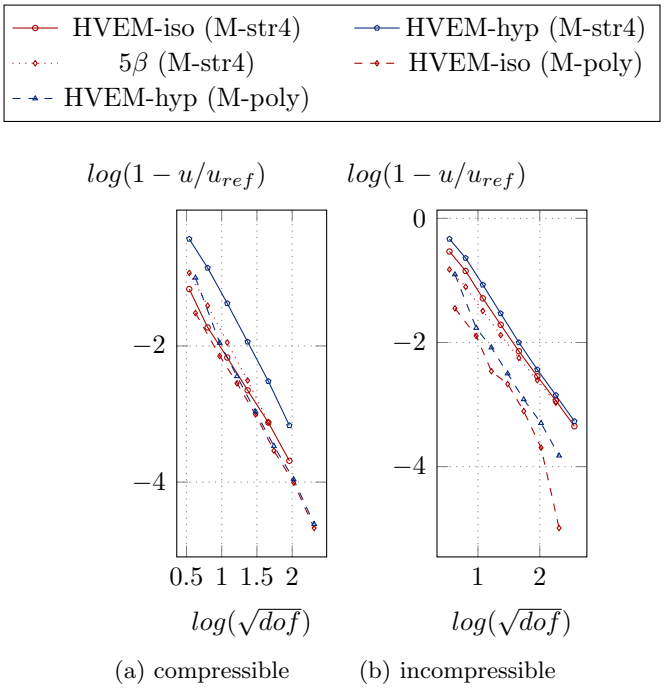

(a) compressible (b) incompressible

Figure 2: Cook's membrane: convergence curves for structures meshes using different VEM and FEM formulations, compressible (a) and incompressible (b) cases.

7 CONCLUSIONS

This work establishes that the minimization of Total Potential Energy and the projection operation typical of the enhanced Virtual Element Method can be derived from the stationarity condition of the Hellinger-Reissner mixed functional. This insight led to the development of the Hybrid Virtual Element Method (HVEM), a family of polygonal elements for plane elasticity problems that can function as either virtual elements or hybrid finite elements. In HVEM, stability is achieved through carefully selected stress fields, using two stabilization-free concepts: *hyper-stability*, which ensures stress interpolation completeness, and *iso-stability*, which optimizes the stress interpolation with minimal parameters. Numerical results indicate that the iso-stable HVEM provides higher accuracy, particularly with coarse meshes, though it requires careful selection of the stress interpolation basis. As the mesh is refined, the accuracy and convergence rates of both iso-stable and hyper-stable HVEM become comparable. Additionally, polygonal HVEM outperforms quadrilateral meshes, highlighting an advantage of the polygonal discretization.

REFERENCES

[1] F. Brezzi, R. S. Falk, and L. D. Marini, "Basic principles of mixed virtual element methods," *ESAIM Math. Model. Numer. Anal.*, vol. 48, no. 4, pp. 1227–1240, 2014.

[2] L. Beirão da Veiga, F. Brezzi, and L. D. Marini, "Virtual elements for linear elasticity problems," *SIAM J. Numer. Anal.*, vol. 51, no. 2, pp. 794–812, 2013.

[3] E. Artioli, L. Beirão da Veiga, C. Lovadina, and E. Sacco, "Arbitrary order 2D virtual elements for polygonal meshes: Part I, elastic problem," *Computational Mechanics*, pp. doi:10.1007/s00466–017–1404–5, 2017.

[4] A. Cangiani, G. Manzini, A. Russo, and N. Sukumar, "Hourglass stabilization and the virtual element method." to appear, 2015.

[5] E. Artioli, L. Beirão Da Veiga, C. Lovadina, and E. Sacco, "Arbitrary order 2D virtual elements for polygonal meshes: Part II, inelastic problems," *Computational Mechanics*, pp. DOI 10.1007/s00466–017–1429–9, 2017.

[6] M. L. D. Bellis, P. Wriggers, B. Hudobivnik, and G. Zavarise, "Virtual element formulation for isotropic damage," *Finite Elements in Analysis and Design*, vol. 144, pp. 38 – 48, 2018.

[7] P. Wriggers, W. T. Rust, and B. D. Reddy, "A virtual element method for contact," *Computational Mechanics*, vol. 58, pp. 1039–1050, Dec 2016.

[8] E. Benvenuti, A. Chiozzi, G. Manzini, and N. Sukumar, "Extended virtual element method for two-dimensional linear elastic fracture," *Computer Methods in Applied Mechanics and Engineering*, vol. 390, p. 114352, Feb. 2022.

[9] S. Marfia, E. Monaldo, and E. Sacco, "Cohesive fracture evolution within virtual element method," *Engineering Fracture Mechanics*, vol. 269, p. 108464, jun 2022.

[10] L. Beirão da Veiga, C. Lovadina, and A. Russo, "Stability analysis for the virtual element method," *Mathematical Models and Methods in Applied Sciences*, vol. 27, pp. 2557–2594, Oct. 2017.

[11] A. D'Altri, S. de Miranda, L. Patruno, and E. Sacco, "An enhanced vem formulation for plane elasticity," *Computer Methods in Applied Mechanics and Engineering*, vol. 376, p. 113663, Apr. 2021.

[12] M. Cremonesi, A. Lamperti, C. Lovadina, U. Perego, and A. Russo, "Analysis of a stabilization-free quadrilateral Virtual Element for 2D linear elasticity in the Hu-Washizu formulation," *Computers & Mathematics with Applications*, vol. 155, pp. 142–149, Feb. 2024.

[13] E. Artioli, S. de Miranda, C. Lovadina, and L. Patruno, "A family of virtual element methods for plane elasticity problems based on the Hellinger–Reissner principle," *Computer Methods in Applied Mechanics and Engineering*, vol. 340, pp. 978–999, 2018.

[14] E. Artioli, S. de Miranda, C. Lovadina, and L. Patruno, "A stress/displacement Virtual Element method for plane elasticity problems," *Computer Methods in Applied Mechanics and Engineering*, vol. 325, pp. 155–174, 2017.

[15] A. Lamperti, M. Cremonesi, U. Perego, A. Russo, and C. Lovadina, "A Hu–Washizu variational approach to self-stabilized virtual elements: 2D linear elastostatics," *Computational Mechanics*, vol. 71, pp. 935–955, Feb. 2023.

[16] A. Chen and N. Sukumar, "Stress-hybrid virtual element method on quadrilateral meshes for compressible and nearly-incompressible linear elasticity," 2023.

[17] T. Pian and K. Sumihara, "Rational approach for assumed stress finite elements," *International Journal for Numerical Methods in Engineering*, vol. 20, no. 9, p. 1685 – 1695, 1984.

[18] A. Madeo, G. Zagari, and R. Casciaro, "An isostatic quadrilateral membrane finite element with drilling rotations and no spurious modes," *Finite Elements in Analysis and Design*, vol. 50, pp. 21–32, 2012.

[19] S. Cen, X.-R. Fu, and M.-J. Zhou, "8- and 12-node plane hybrid stress-function elements immune to severely distorted mesh containing elements with concave shapes," *Computer Methods in Applied Mechanics and Engineering*, vol. 200, no. 29, pp. 2321–2336, 2011.

[20] S. de Miranda and F. Ubertini, "A simple hybrid stress element for shear deformable plates," *International Journal for Numerical Methods in Engineering*, vol. 65, no. 6, pp. 808–833, 2006.

[21] A. Madeo, F. S. Liguori, G. Zucco, and S. Fiore, "An efficient isostatic mixed shell element for coarse mesh solution," *International Journal for Numerical Methods in Engineering*, vol. 122, no. 1, pp. 82–121, 2021.

[22] F. S. Liguori and A. Madeo, "A corotational mixed flat shell finite element for the efficient geometrically nonlinear analysis of laminated composite structures," *International Journal for Numerical Methods in Engineering*, vol. 122, no. 17, pp. 4575–4608, 2021.

[23] F. S. Liguori, A. Madeo, and G. Garcea, "A dual decomposition of the closest point projection in incremental elasto-plasticity using a mixed shell finite element," *International Journal for Numerical Methods in Engineering*, vol. 123, no. 24, pp. 6243–6266, 2022.

[24] Z. She, K. Wang, and P. Li, "Hybrid Trefftz polygonal elements for heat conduction problems with inclusions/voids," *Computers & Mathematics with Applications*, vol. 78, no. 6, pp. 1978–1992, 2019.

[25] F. Liguori, A. Madeo, S. Marfia, and E. Sacco, "A hybrid virtual element formulation for 2d elasticity problems," *Computer Methods in Applied Mechanics and Engineering*, vol. 426, p. 116970, 2024.

[26] F. Liguori, A. Madeo, S. Marfia, G. Garcea, and E. Sacco, "A stabilization-free hybrid virtual element formulation for the accurate analysis of 2d elasto-plastic problems," *Computer Methods in Applied Mechanics and Engineering*, vol. 431, p. 117281, 2024.

[27] A. Bilotta and R. Casciaro, "Assumed stress formulation of high order quadrilateral elements with an improved in-plane bending behaviour," *Computer Methods in Applied Mechanics and Engineering*, vol. 191, no. 15, pp. 1523–1540, 2002.

[28] G. Zucco, R. Groh, A. Madeo, and P. Weaver, "Mixed shell element for static and buckling analysis of variable angle tow composite plates," *Composite Structures*, vol. 152, pp. 324–338, 2016.